Non-stationarities in the relationships of heavy precipitation events in the Mediterranean area and the large-scale circulation in the second half of the 20th century

Christian Merkenschlager, Elke Hertig, Jucundus Jacobeit

Angaben zur Veröffentlichung / Publication details:

Merkenschlager, Christian, Elke Hertig, and Jucundus Jacobeit. 2017. "Non-stationarities in the relationships of heavy precipitation events in the Mediterranean area and the large-scale circulation in the second half of the 20th century." *Global and Planetary Change* 151: 108–21. https://doi.org/10.1016/j.gloplacha.2016.10.009.

Non-stationarities in the relationships of heavy precipitation events in the Mediterranean area and the large-scale circulation in the second half of the 20th century

Christian Merkenschlager *, Elke Hertig, Jucundus Jacobeit

Institute of Geography, University of Augsburg, Alter Postweg 118, 86159 Augsburg, Germany

1. Introduction

Since Giorgi (2006) characterized the Mediterranean area as one of the main climate change hot-spots whose climate responds more sensitive to global climate change compared to other regions, many studies had put their emphasis on the relevant processes and physical mechanisms to understand the variability of climate parameters like precipitation (e.g. Kelley et al., 2012; Lionello et al., 2014; Mariotti and Dell'Aquila, 2012), their impacts on the socio-economic structure (e.g. Iglesias et al., 2007; Latorre et al., 2001; Stefanova et al., 2015) and the terrestrial ecosystems (e.g. Batllori et al., 2013; Filipe et al., 2013; Henne et al., 2013) in this region in a changing climate. But comparisons of the modeled and the observed precipitation of the Mediterranean area offer significant contradictions especially in the seasonal cycle. For winter season Barkhordarian et al. (2013) assume that shifts of the large-scale circulation have influence on the significant underestimation of the climate change signal in this region. Since the Mediterranean area lies in a transition zone between the humid climate of Central and Western Europe and the arid climate of North Africa where different large-scale circulation modes are predominant (Dünkeloh and Jacobeit, 2003; Giorgi and Lionello, 2008), a shift of the large-scale circulation within global

Abbreviations: BS, Brier Score; BSS, Brier Skill Score; CQR, censored quantile regression; CQVS, censored quantile verification score; CQVSS, Censored Quantile Verification Skill Score; EM, Eastern Mediterranean; EMULATE, European and North Atlantic daily to MULtidecadal climATE variability; GLM, generalized linear model; GLOWA, Global Change and the Hydrological Cycle; HGT, geopotential heights; IID, independently identically distributed; LAD, least absolute deviation; MO, Mediterranean Oscillation; NCAR, National Center for Atmospheric Research; NCEP, National Centers for Environmental Prediction; PC, principal component; PCA, principal component analysis; PCS, principal component scores; POT, peak over threshold; PPP, Poisson point process; PR, precipitation region; QR, quantile regression; RHUM, relative humidity; SHUM, specific humidity; TSCQR, three-step censored quantile regression; UWND, zonal wind component; VWND, meridional wind component; WM, Western Mediterranean.

* Corresponding author.

E-mail addresses: christian.merkenschlager@geo.uni-augsburg.de (C. Merkenschlager), elke.hertig@geo.uni-augsburg.de (E. Hertig), jucundus.jacobeit@geo.uni-augsburg.de (J. Jacobeit).

climate change has a significant impact on total precipitation amounts and extremes all over the Mediterranean area and therefore impacts on the water availability and the terrestrial ecosystems as well.

In a complex terrain like the Mediterranean area where the topography has a great influence on the observed structure of weather systems and the regional circulation (Fernandez et al., 2003), precipitation events, especially extreme events, often occur on a small regional scale. The topography also induces fine scale features which have impacts on the precipitation change signal over the Mediterranean region (Gao et al., 2006). Hence, global climate models with their sparse horizontal resolution are unable to fully capture and assess those local weather events (Friederichs and Hense, 2008). Nevertheless, a significant fraction of the large spatio-temporal variability of winter time precipitation is related to advective processes which can be described by the large-scale circulation (Xoplaki et al., 2004). For this reason, only statistical and dynamical downscaling methods which combine the local conditions with the large scale circulation can provide reliable assessments of local weather characteristics and their variability within a changing climate (Friederichs and Hense, 2008).

Several studies based on different downscaling techniques project decreasing precipitation amounts for the southern and eastern parts of the Mediterranean area while precipitation totals of the western and northern parts are increasing (e.g. Hertig et al., 2012). In contrast to precipitation totals, projections of precipitation extremes are less conclusive because the results strongly depend on the model, the type of extreme and the region of the Mediterranean area (Hertig and Jacobeit, 2014; Toreti and Naveau, 2015). It is assumed that in many regions the total precipitation sums tend to decrease while extreme precipitation events will increase (Alpert et al., 2002). However, Hertig et al. (2012) showed that areas with mean precipitation being reduced and extreme precipitation being increased are not that common and thus might not be the dominant mode of change in the Mediterranean area. Furthermore, Toreti and Naveau (2015) showed that heavy precipitation events will increase till the end of the 21st century, but the behavior of the tails of the distribution differs, depending on the examined region or model, and is characterized by a high uncertainty. Overall, the precipitation totals of the Mediterranean area are characterized by great space-time variability where the number of precipitation events will decrease but the intensity of rainfall events will increase causing longer lasting within-season drought and changes in evapotranspiration and greater surface runoff (Maccracken et al., 2003). Because most of the precipitation is generated in winter where westward moving storms convey humidity to the Mediterranean basin, winter time precipitation is essential for the water budget in this area (Hertig and Jacobeit, 2014). For this reason only winter season is considered within this study although precipitation events of the transitional seasons, especially in the northern parts of the Mediterranean area, should clearly kept in mind in matters of the water management.

One of the major problems of estimating daily precipitation amounts is that precipitation is not Gaussian but a non-negative mixed discrete-continuous variable where no general agreement exists which distribution fits best (Friederichs and Hense, 2007). Therefore, within the range of statistical downscaling different methods like perfect prog (e.g. Klein, 1971), model output statistics (e.g. Glahn and Lowry, 1972) or a combination of both methods (Marzban et al., 2006) were applied on estimating daily precipitation sums (Friederichs and Hense, 2008). An alternative method is called quantile regression which was established by Koenker and Bassett (1978) and first applied to climate studies by Bremnes (2004). Since precipitation is a non-negative variable with a lower bound of zero it is a so-called censored variable (Friederichs and Hense, 2007). For quantile regression of censored variables two different methods are available. First, an algorithm developed by Fitzenberger (1997) called censored quantile regression (CQR) can be adapted on every quantile of interest. An alternative approach, the so-called three-step censored quantile regression (TSCQR), is presented by Chernozhukov and Hong (2002) and is divided into three steps where standard quantile regression is applied on different subsamples depending on the probability of rain and the quantile of interest. A wide range of methods is also available for estimating extremes. A comparison of three different approaches is given by Friederichs (2010). Here, the conditional precipitation quantiles were assessed for different German weather stations by means of 1) a CQR, 2) a Poisson point process model (PPP) and 3) a peak over threshold model (POT). Instead of CQR, the TSCQR can be used for estimating extreme quantiles as well like Friederichs and Hense (2007).

A further method is presented by Hertig and Jacobeit (2014), using generalized linear models based on Tweedie distribution to estimate precipitation extremes in the Mediterranean area. Here, the emphasis is put on the detection and analysis of non-stationarities in the predictor-predictand relationships in order to take them into account for future projections. Non-stationarities occur when the relationships between circulation patterns or centers of variation (predictors) and the target variable like precipitation (predictand) is more weak or intense than it can be explained by natural variability. Non-stationary behavior could either be a matter of physical variations of the circulation or a matter of so-called within-type variations (Beck et al., 2007, Hertig and Jacobeit, 2014). The importance of considering shifts of the large-scale circulation for Mediterranean precipitation projections is underlined by the study of Barkhordarian et al. (2013). The authors find that the observed winter precipitation amounts are subjected to a significant negative trend which cannot be described by the different climate models. It is assumed that shifts of the large-scale circulation are responsible for the differences between the modeled and observed precipitation which are outside the range of natural variability. However, this study is based on projections for the whole Mediterranean area and, hence, no reliable conclusions can be drawn for the influence of the large-scale circulation shifts on precipitation time series on a regional scale where topographic parameters lead to modifications of the climate change signal. For this reason, in order to obtain more confident assessments of precipitation and extremes in the Mediterranean area non-stationary behavior should be taken into account for climate change studies in the Mediterranean area (Hertig and Jacobeit, 2014).

In this study we present a detailed approach to detect and analyze non-stationary behavior within the large-scale circulation-precipitation relationships by means of one reference station of the Mediterranean area where a non-stationarity is highly distinct. For this purpose, we divide the study period into 31-year running subsamples and analyzed them separately. Thus, we not only have one regression model for the whole period, but an ensemble of regression models describing every state of the atmosphere. A comparison of composites should then determine the most suitable regression model to assess heavy precipitation events under changing climate conditions in the future. Thus, the assessment of heavy precipitation events is performed under the explicit consideration of non-stationary behavior of large-scale circulation-precipitation relationships.

Section 2 describes pre-processing and regionalization of the station data and some selection criteria for the variables of the reanalysis data set. In Section 3 a brief overview of the TSCQR and the CQVSS is given followed by a detailed description of the predictor selection and the analyzing methods. The results for the reference stations in matters of predictor selection and non-stationarities are illustrated in Section 4 followed by a more detailed description of the methods and an analysis of composites by means of an example station (Safed, Israel) where a medium negative non-stationarity (see Section 3.4) is supposed. In Section 5 we draw some conclusions of the major findings. In this study the emphasis is put on the detection of non-stationarities and the analysis of composites, assessments for future periods are not the scope of this paper.

2. Data

2.1. Predictand

Daily precipitation time series of over a hundred stations of the Mediterranean area have been collected from the European Climate Assessment & Dataset (Klein Tank et al., 2002), from the GLOWA Jordan River Project (Global Change and the Hydrological Cycle, Kunstmann et al., 2006), and from the EMULATE project (European and North Atlantic daily to MULtidecadal climATE variability, Moberg et al., 2006). The datasets comprise more or less the years from the mid 20th to the early 21st century with a minimum number of 41 years. The threshold of 41 years is attributed to an adequate length of the calibration period (31 years) and at least ten years of validation. The longest time series contain 59 years from 1950 to 2008 and all station time series contain the period of 1961 to 1990. Most of the Mediterranean area is well covered by the available datasets, especially the Iberian Peninsula and the Levant region, only in the southern region (notably Northern Africa) and in parts of the north-eastern Mediterranean area (Turkey) a lack of data is located.

In a first step the station data was tested on completeness and homogeneity. The annual data sets were split into seasons and winter season (December to February) was extracted. For convenience, December is always assigned to the following year. This means that in all figures and annotations for example the winter season of 1967/68 is denoted as winter 1968. The test on completeness follows an approach of Moberg and Jones (2005) and is subject to three conditions. First, a month is considered to be complete when there are less than three missing days. If every month of a year is complete, the year is considered to be complete as well. But in contrast to the approach of Moberg and Jones (2005), condition three was applied to the whole time series instead of 20 year blocks. In summary, 94 stations of the Mediterranean area were classified as complete for at least 41 years. Subsequently, based on an approach of Wijngaard et al. (2003) and Alexandersson (1986) the station data were tested on homogeneity. Here, the station data were subjected to five different homogeneity tests, four absolute and one relative homogeneity test. The test developed by Alexandersson (1986) can be used relatively as well as absolutely and originally is appropriate for detecting single breaks. Here, an extended version of this testing method was applied on the station data which is able to capture multiple breaks. The other absolute testing methods are the Pettitt test (Pettitt, 1979), the Buishand range test (Buishand, 1982) and the von Neumann ratio test (von Neumann, 1941). Similar to Wijngaard et al. (2003) the results were grouped into three categories. If one or fewer tests signals an inhomogeneous behavior of the station data the dataset was classified as "useful", if two homogeneity tests failed the station was classified as "doubtful" and if more than two tests failed the station was categorized as "suspect".

Within this approach the number of wet days is taken into account, and only days with daily precipitation sums over 1 mm are considered as wet days. The number of wet days is more suitable for homogeneity tests than the annual precipitation sums, because of the lower variability. This leads to a reduction of noise and, thus, not only inhomogeneities of a larger extend are detectable (Wijngaard et al., 2003).

In order to generate precipitation regions of the Mediterranean area with similar precipitation variability an s-mode, varimax-rotated principal component analysis (PCA, e.g. Preisendorfer, 1988; Richman, 1986) was applied to the data sets of the weather stations. The number of extracted principal components (PCs) results from two criteria. First, the absolute maximum PC loading of at least two stations is assigned to every PC. Second, the highest absolute maximum loading exceeds 0.7. 22 PCs with an overall explained variance of 74.8% were obtained from this PCA for winter season. The different precipitation regions are shown in Fig. 1. The different colors represent the precipitation regions, whereas diamonds point out the reference stations. The reference stations of the different PCs were selected by choosing a time series with almost homogeneous behavior, an appropriate length and a relative high loading. The first criterion for selecting the reference station is the loading of a time series according to the respective PC. But if the station with the highest loading failed to more than one homogeneity test or a station with almost similar high maximum PC loading comprises more years, we choose the second station as reference station. The maximum loadings of the stations range from 0.4031 to 0.9438, the maximum loadings of the reference stations from 0.5897 to 0.9438. Overall, 65 stations show no inhomogeneous behavior at all, 21 stations are useful but failed to one test and 8 stations are doubtful or suspect, but only one precipitation region (PC-17) exists where all stations are doubtful or suspect and, thus, the results have to be considered with care for this region. All subsequent analyses are related to the reference stations of the different PCs.

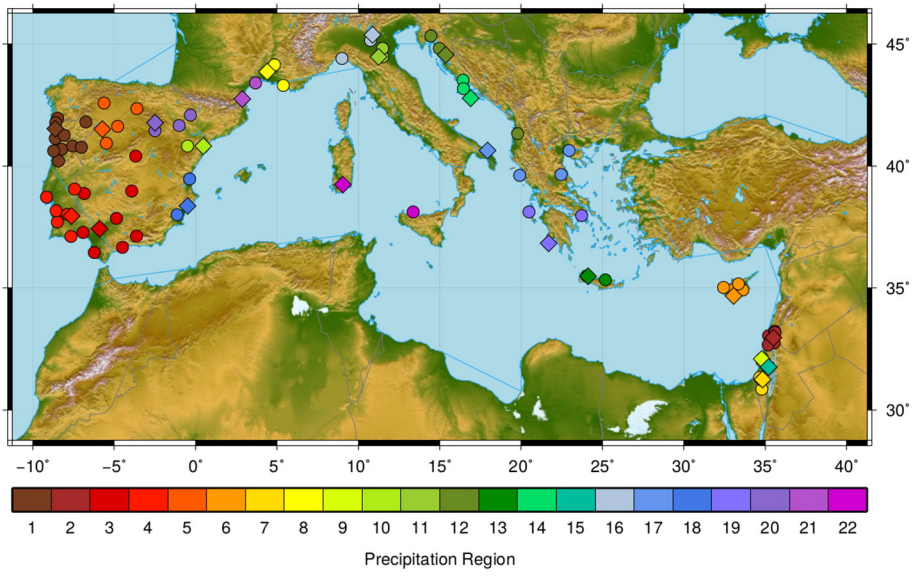

Fig. 1. Precipitation regions of the Mediterranean area in winter. The diamonds represent the reference stations of the respective precipitation region and the circles the corresponding stations.

2.2. Predictor

Various variables of the widely-used NCEP/NCAR reanalysis data set (Kalnay et al., 1996; Kistler et al., 2001) were used as predictors. The daily reanalysis data are available on a 2.5°×2.5° grid and the length is adapted to the length of each station time series. Earlier analyses had shown, that the thermodynamic variables of the 850 hPa level and the circulation-dynamic variables of the 700 hPa level play an important role for precipitation in the Mediterranean area during winter time (Hertig and Jacobeit, 2013; Hertig et al., 2014). On the other hand many studies point out that processes of the upper troposphere are important for analyzing precipitation extremes as well (e.g. Massacand et al., 1998; Martius et al., 2008; Toreti et al., 2015). For this reason, the geopotential heights and the relative humidity were tested for three reference stations (Barcelos, Portugal; Gospic, Croatia; Jerusalem, Israel) across the Mediterranean area at all different levels of the NCEP/NCAR reanalysis data set. The CQVSS (see Section 3.2) is calculated for all grid boxes of the chosen domains (see below). It becomes apparent that the relative humidity reaches high values on lower levels (1000 Pa–850 hPa-level) before the scores decrease rapidly. Although the maximum skill scores are not on the 850 hPa-level for all stations, the 850 hPa-level provides adequate scores for most of the stations. The maximum scores of the geopotential heights were reached at higher levels before a strong decrease begins at the 300 hPa-level. As the relative humidity, the geopotential heights reach their maximum not on the same level, but the differences between the maximum scores and the scores of the 700 hPa-level are marginal. Overall, the results of the 850 hPa-level for thermodynamic and the 700 hPa-level for circulationdynamic variables provide proper scores and, thus, are most suitable for further analyses.

For the circulation-dynamic variables, i.e. geopotential heights (hgt), zonal (uwnd) and meridional (vwnd) wind components, a larger domain is chosen (40°W–50°E, 25°N–60°N) than for the thermodynamic variables like specific (shum) and relative (rhum) humidity (10°W–40°E, 27,5°N–45°N). In summary, five different variables on two different levels were taken into account as predictors for the regression models. Subsequently, an s-mode varimax-rotated PCA is applied to the different predictor variables to obtain centers of variations. Depending on the predictor variable the cumulative explained variance varies from 73.4% (relative humidity at 850 hPa) to 90.6% (geopotential heights at 850 hPa) and the number of extracted PCs from 9 (zonal wind at 850 hPa) to 16 (rhum at 850 hPa).

3. Methodology

3.1. Three-step censored quantile regression

A three-step censored quantile regression (TSCQR) is used to estimate the precipitation quantiles. This method was developed by Chernozhukov and Hong (2002) for studies on extramarital affairs and then transferred by Friederichs and Hense (2007) to studies on extreme precipitation events over Germany. They had shown, that a censored quantile regression is appropriate for modeling a mixed discrete-continuous response variable like daily precipitation sums. The TSCQR is an alternative approach for the censored quantile regression, which was established by Koenker and Bassett (1978). A comparison of both methods is mentioned in Friederichs and Hense (2007). Both methods provided almost identically estimates of the conditional quantiles, but the TSCQR requires less computational time than the censored quantile regression.

The first step of the TSCQR is to estimate the probability of rain for every day of the period by means of the significant predictors. For the assessment of the probability of rain a generalized linear model (GLM) in terms of a logit function was used. For every day of the period we obtain the probability of rain. Based on this estimate a subsample S_1 is chosen with all days, with an estimated value exceeding $1-\tau$, where τ is the quantile of interest. In a second step, an initial estimation of the β-coefficients based on the subsample S_1 is realized by means of standard quantile regression. Standard quantile regression is part of the R package quantreg developed by Koenker (2013) . The advantage of quantile regression (QR) in contrast to standard regression is that QR uses the least absolute deviations (LAD) to estimate the β-coefficients and only assumes an independently identically distributed (IID) error (Friederichs and Hense, 2007; Koenker, 2005). The β-coefficients were estimated by means of the subsample S_1 and then transferred to the whole period of interest. Thus, a quantile value is calculated for all days of the period which describes the threshold of daily precipitation sums which is not exceeded in $\tau * 100\%$ of all cases. Because negative quantile values are possible as well, a third step, representing the censoring, is necessary. An updated subsample S_2 is chosen with all days, which estimated quantile values are greater than zero. Here, the zero precipitation line stands for the censor. Then, a standard quantile regression is applied on the new subsample S_2, again. Subsequently, the quantiles can be modeled by means of the three-step β-coefficients, where still some values can be smaller than zero. If the number of days with quantiles smaller than zero is still high, a rerun of step three is recommended. Otherwise, the remaining days with quantiles smaller than zero are set to zero. Detailed explanations of the three-step censored quantile regression are given in Chernozhukov and Hong (2002) and, for climate related applications, in Friederichs and Hense (2007).

3.2. Validation

Two different methods were used to estimate the skill of the established models. On the one hand we used the Brier Skill Score (BSS) to determine the quality of the logit model. For this purpose, the averaged mean squared error of the probability forecast is calculated (BS_{mod}), considering that the observations are assigned a value $o_i = 1$ if the event occurs, and $o_i = 0$ if the event does not occur. The Brier score of the reference (BS_{ref}) is obtained by using the probability of the climatology instead of the forecast p_i.

$$BS_{mod} = \frac{1}{N}\sum_{i=1}^{N}(p_i - o_i)^2$$

Hence, the BSS is:

$$BSS = 1 - \frac{BS_{mod}}{BS_{ref}}$$

The Brier Skill Score is a well-established method to test the quality of binary events and was used (e.g. Hertig and Jacobeit, 2014; Friederichs and Hense, 2007) and explained (e.g. Wilks, 2011) in many publications before.

On the other hand, the Censored Quantile Verification Skill Score (CQVSS or QVSS in other publications), established by Friederichs and Hense (2007) is used as a measure of goodness for the TSCQR. To obtain the censored quantile verification score of our model ($CQVS_{mod}$) as a function of τ, the difference of the observation (y_i) and the respective modeled quantile value (q_{τ_i}) had to be generated

$$CQVS_{mod} = \sum_{i=1}^{N}\rho_\tau\left(y_i - q_{\tau_i}\right)$$

under consideration of the so-called check function

$$\rho_\tau(u) = \begin{cases} \tau u & \text{if} \quad u \geq 0 \\ (\tau - 1)u & \text{if} \quad u < 0. \end{cases}$$

As reference the modeled quantile value is replaced by the corresponding value of the climatological distribution of the observation.

Thus, the CQVSS for a specific τ is:

$$CQVSS(\tau) = 1 - \frac{CQVS_{mod}(\tau)}{CQVS_{ref}(\tau)}$$

For both skill scores a zero skill score denotes no gain in predictive skill. If the skill score is less than zero, the model is worse than the climatology, whereas a value greater than zero denotes an improvement. The selection of the predictors and the identification of non-stationarities is mostly based on the calculation of the CQVSS (see Sections 3.3 and 3.4).

3.3. Predictor selection

In a first step all different combinations of two predictor variables of both levels were taken into account in order to obtain the best combination of variables with the highest skill score. TSCQR was applied on the whole period in order to reproduce the time series of the weather stations. In most instances, a combination of one thermodynamic and one circulation-dynamic variable provides the best scores. The score was calculated by means of all PCs of both variables, which are significant at a level of $\alpha = 0.01$. Under consideration of a third predictor variable the CQVSS shows only little improvements at all stations so that a third variable can be disregarded. Overall, 40 variable combinations were possible when the combination of the same variable at different levels was skipped. For each station the predictor combination with the highest CQVSS was determined and used for further analyses.

After identifying the best variable combination we had to select the significant PCs. 100 random sampled 31-year time series were drawn from the whole period. Now, the model was set up for each random sampled time series considering only those PCs which were significant at a level of $\alpha = 0.01$. The significant PCs varied according to the selected years with only a small number of PCs, which were significant in most of the cases. If a PC was classified as significant in at least 95% of all cases the PC was considered for further analyses. A threshold of 95% was chosen because the selection runs more stable than with a threshold of 100%. Furthermore, considering centers of variation which are not relevant in all but most of the cases led to a significant improvement of the scores without the risk of overfitting.

3.4. Detection of non-stationarities

In order to assess model performance under non-stationary and under stationary conditions, we followed two different approaches (Hertig and Jacobeit, 2014). To check the performance under stationary conditions the whole time series was split into a calibration and a validation period. 100 random samples, containing 31 years, were drawn from the station data, which represent the calibration periods. Subsequently, a TSCQR is applied on every calibration period in order to assess the τ-th quantile of all validation periods by means of the obtained β-coefficients. In addition, we estimated the CQVSS for all of the 100 random samples. The highest and lowest CQVSS out of the 100 random samples were taken to define the interval of random variability.

The other approach depicts the model performance under non-stationary conditions. The available station time series were split into 31-year running calibration periods and the remaining years were used as validation period in each case. Thereby, the calibration period was shifted throughout the whole time series by one year and when the end of the time series was reached, years from the beginning were added to avoid a weighting in favor of the middle years. The CQVSS from a validation period was assigned to the middle year of the respective calibration period in order to receive a CQVSS time series. This approach guarantees that observed inter-annual or decadal variability and trends are preserved and potential temporal non-stationarities could still be identified (Hertig and Jacobeit, 2014).

By means of the thresholds derived from the random sampling and the time series of our skill score derived from the running sub-intervals, a non-stationarity was defined if several consecutive years are outside the range of random variability of the skill score. We only consider non-stationarities with more than three consecutive years outside this range and relate them to different classes. If the number of consecutive years outside the thresholds ranges between three and five a small non-stationarity is declaimed. A medium non-stationarity exists when up to ten consecutive years are outside the borders and a large one when more than ten consecutive years are outside the given interval. Another differentiating factor is whether the time series falls below the lower boundary (negative non-stationarity) or exceeds the upper boundary (positive non-stationarity). For example, a large negative non-stationarity indicates a period where the relationships between the large-scale circulation and precipitation are more weak for at least ten consecutive years in comparison to the remaining time series.

3.5. Analysis of non-stationarities

If a time series contains a certain period of time with non-stationary behavior we try to gain insight to the physical background of the predominant large-scale circulation. Composites were computed for the respective predictors of the periods with the highest and lowest CQVSS. Here, only those years were taken into account which are explicitly part of the respective validation period, because only difference within these periods are responsible for the non-stationarities between the large-scale circulation and the daily precipitation amounts. The different periods were denoted as $CQVSS_{MIN}$ and $CQVSS_{MAX}$. The denoted subset $CQVSS_{MAX}$ ($CQVSS_{MIN}$) conforms to the validation period of $CQVSS_{MIN}$ ($CQVSS_{MAX}$). Subsequently, composites were computed where the daily scores of the significant predictors exceed or fall below a certain threshold. Especially subsamples of days with PC scores (PCS) greater/smaller ± 2.0 are relevant because in this case the PCs are highly distinct. For these days the mean scores and absolute values of the significant PCs as well as absolute and standardized values of the geopotential heights and the wind parameters were averaged to emphasize regime anomalies.

Analyses are based on comparisons of the whole periods of $CQVSS_{MIN}$ and $CQVSS_{MAX}$. Here, especially numerical parameters like how many precipitation events occur within these periods, the extent of the mean total precipitation amounts per season, per day or event, and the number of days exceeding a certain threshold was analyzed. A numerical evaluation of the different composites with PCS exceeding/falling below a certain threshold is done as well. Finally, the geopotential heights, the anomalies and the wind fields were analyzed in order to detect differences of the large-scale circulation between $CQVSS_{MIN}$ and $CQVSS_{MAX}$.

4. Results

4.1. Predictor selection

For predictor selection the best combination of two predictor variables considering only those PCs of both sets which are significant at a level of $\alpha = 0.01$, were used to reproduce the whole time series of the reference stations. The inclusion of a third predictor variable resulted in an improvement of the CQVSS not >0.05 and thus, in order to avoid overfitting of the model setup through too many predictors, the consideration of a third predictor was dismissed. In general, a combination of one predictor representing the circulation-dynamic and one predictor representing the thermodynamic aspects provides the highest CQVSS. For $\tau = 0.90$, relative humidity (850 hPa- or 700 hPa-level) is representative for the thermodynamic variables in 82% of all cases, while in 55% of all cases the zonal wind component (both levels), and in 41% the meridional wind component (both levels) constitutes the circulation-dynamic variable. A preferred level cannot be identified for the different predictor combination, most of the predictor combinations contain both levels. For all precipitation regions we obtain BSSs and CQVSSs

greater than zero with BSSs between 0.2874 for precipitation region (PR) 18, represented by Alicante (Spain) and 0.7466 for PR-1, represented by Barcelos (Portugal) and with CQVSSs between 0.2634 for PR-18 and 0.5239 for PR-3, represented by Sevilla (Spain). From PR-18 which has the lowest BSS as well as the lowest CQVSS it might be assumed that there is a correlation between the results of the logit model and the skill scores of the quantile regression, but a weaker logit model does not compulsorily lead to weaker estimations of the censored quantile regression. However, a high (low) BSS will not result in a low (high) CQVSS but in between no statistical inference can be drawn from the BSSs. The composition of the predictor variables are displayed in Fig. 2. Here, the first predictor variable is represented by the shape of the symbols, the second variable by the color of the symbols, with the first predictor variable being the PC with the highest regression coefficient.

Subsequently, the selection of the significant PCs of the best variable combination was done by means of cross validation. 100 random sampled 31-year calibration periods were drawn from the whole period while the rest of the station time series years represent the validation period. If a PC is significant at a level of $\alpha = 0.01$ in 95% of all random samples the PC was considered for model setup. The established models (logit- and TSCQR-model) were then transferred to the validation period. Both scores slightly decrease in comparison to the reproduction of the whole time series but the loss of skill averages 0.0160 (BSS) respectively 0.0306 (CQVSS). The greatest decrease of skill can be observed for PR-18 (Alicante, Spain) with 0.0274 for the BSS and PR-21 (Perpignan, France) with 0.0624 for the CQVSS whereas PR-2 (Safed, Israel) with 0,0071 (BSS) and PC-20 (Soria, Spain) with 0,0115 (CQVSS) have only a marginal loss of skill.

For the 90th quantile the number of significant PCs varies from 2 to 8 and is depicted as symbol size in Fig. 2. Overall, a spatial pattern of the variable combination and number of significant PCs is not distinct in Fig. 2.

4.2. Detection of non-stationarities

For the stationary models which are used to obtain the upper and lower boundary of the natural variability range and for the running subintervals only the significant centers of variation are taken into account. Overall, we found 9 precipitation regions with non-stationary behavior, 4 precipitation regions with positive (yellow), 5 regions with negative (magenta) non-stationarities (Fig. 2). Here, one positive (PR-21) and one negative (PR-17) non-stationarities were assigned to large non-stationarities (>10 years), one positive (PR-14) and three negative (PR-2, PR-11, PR-15) non-stationarities are of medium extent (6–10 years) and one negative (PR-9) and two positive (PR-3, PR-4) non-stationarities comprise <3 to 5 years. The duration of the non-stationarity is represented by the outline width of the symbols in Fig. 2. Remarkably is, that the detected non-stationarities in the western parts of the Mediterranean area are positive while the non-stationarities of the eastern Mediterranean are negative. An indefinite structure with negative and positive non-stationarities exists in the central parts of the Mediterranean regions.

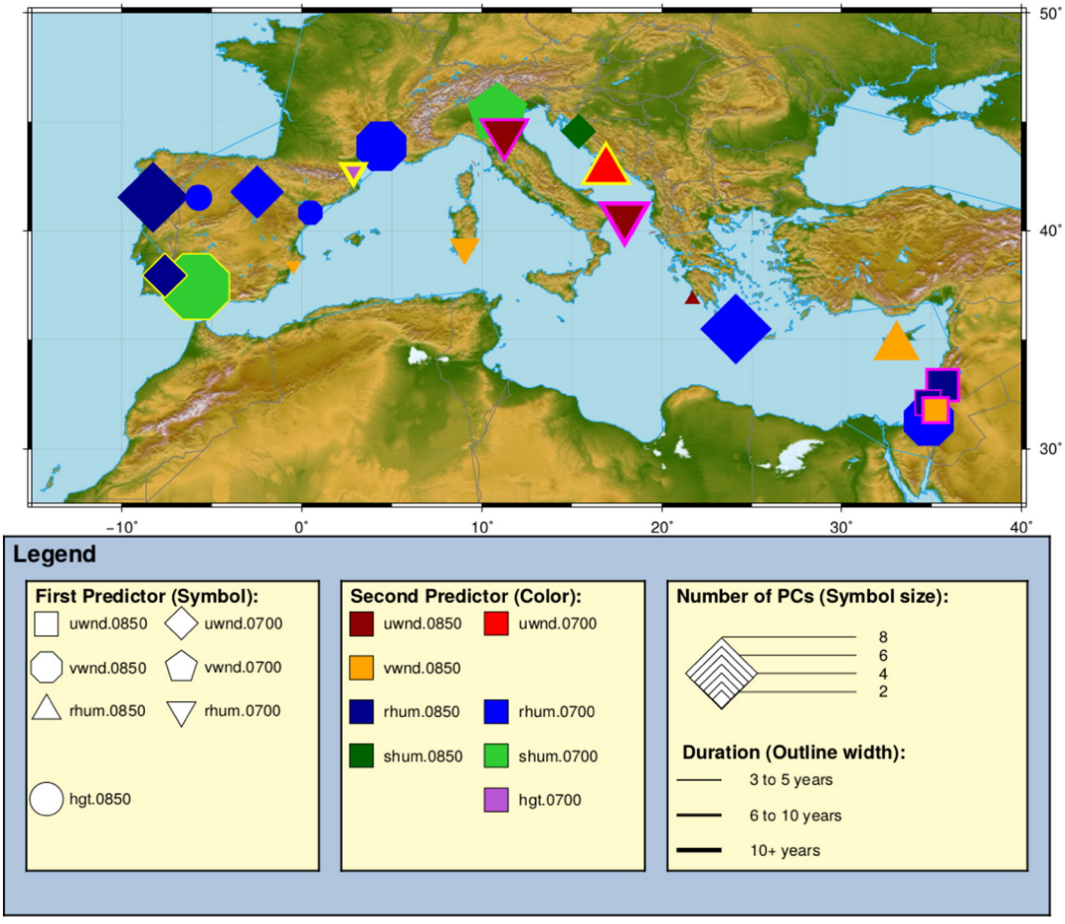

Fig. 2. Predictor combination, number of predictors, duration and type of non-stationarity of the 22 reference stations for the winter season. The symbol characterizes the first predictor variable with the highest skill score for the 90th quantile of the respective station, the color represents the second predictor variable. The size of the symbols illustrates the number of significant principal components (PCs). The color of the outlines determines the type of non-stationarity (positive: yellow; negative: magenta). The outline width defines a small (thin), medium (normal) or large (thick) non-stationarity. Symbols without outline denote no non-stationary behavior. (For interpretation of the references to color in this figure legend, the reader is referred to the web version of this article.)

The correlation coefficients between BSS and CQVSS of the running subintervals show a large spread due to the explained variance for the different stations. The highest correlation coefficients are reached for stations in Israel with an explained variance of over 90% for PR-15 (Jerusalem, $r = 0.9797$) and PR-2 (Safed, $r = 0.9673$). Both stations also show negative non-stationary behavior which leads to the assumption that changes of the large-scale circulation lead to decreasing skill in estimating rainfall probability and, thus, decreasing skill in estimating heavy precipitation events. Even the largest negative non-stationarity of PR-17 (Brindisi, Italy) is for the most parts a result of decreasing skill in estimating rainfall probability ($r = 0.7540$). Nevertheless, a high correlation coefficient of BSS and CQVSS is no evidence of non-stationary behavior, because many stations without non-stationarities have high correlation coefficients as well. For positive non-stationarities only one precipitation region can be assigned to a lack of estimating rainfall probability (PR-4, $r = 0.8036$). The other stations with non-stationary behavior (positive or negative) are more or less affected by decreasing skill of the logit model but there are other effects as well which have a certain influence. Below, a case study is given for the detection and analyses of non-stationary behavior.

4.3. Non-stationary behavior of precipitation using the example of Safed weather station (PR-2)

Safed is a city in the north-eastern part of Israel, 840 m above sea level and about 50 km away from the coast. For this reason, Safed is a city of the more humid part of Israel since rainfall amounts are higher in northern, orographic benefited regions close to the Mediterranean Sea (Saaroni et al., 2010). The available data set comprises homogeneous (no test failed) daily precipitation amounts of 46 years (1958–2003) without any missing data. In Fig. 3 the climatology of Safed weather station in matters of seasonal precipitation amounts, number of wet days and number of wet days exceeding the 90th quantile per year as well as the precipitation amounts per wet day and year is presented. On the left side of Fig. 3 the absolute values, and on the right side the mean deviations are shown with blue colors for $CQVSS_{MIN}$, red colors for $CQVSS_{MAX}$ and gray colors for the overlapping period. The dashed black line, respectively, characterizes the mean values. The mean values per season over the whole study period are: 443.8 mm precipitation; 33.7 wet days; 9.0 wet days exceeding the 90th quantile; 13,1 mm precipitation/wet day. Here, only heavy precipitation events of the 90th quantile were estimated for winter season (winter 1958/59–2002/03). Safed is used for the case study, because of a distinct non-stationarity in the period 1974–83.

4.3.1. Significant centers of variation

For Safed weather station 5 PCs of the zonal wind component (PC-8) and relative humidity (PC-2, PC-9, PC-10, PC-14), both on the 850 hPa-level, are significant in 95% of all cases. The different centers of variation as well as the corresponding β-coefficient time series of the sliding subintervals are presented in Fig. 4. Here, only grid boxes with loadings exceeding ± 0.7 on the respective PC are shown. Overall, there are three centers of variation with positive loadings and two centers with negative ones. The two most important centers of variation are both located over the same region. The PC with the highest absolute mean β-coefficient ($+11.32$) is PC-8 of the zonal wind component. The coefficient varies between $+9.97$ in 1988 and $+13.36$ in 1977. The PC is centered over the Sinai Peninsula and ranges from the north-western parts of Egypt to the central part of northern Saudi-Arabia. The center of variation with the second highest absolute mean β-coefficient (Mean: 3.54; Min: 2.24; Max 5.33) is PC-2 of the relative humidity which is centered over the northern border area of Egypt and Libya. Furthermore, the other PCs of relative humidity, PC-10 (-3.11; -4.94; -2.04) covering the eastern part of Turkey, PC-9 (1.81; 0; 3.08) over the northern part of Saudi-Arabia and PC-14 (-2.61; -2.93; -2.16) over the Mediterranean Sea between Crete and Cyprus affect precipitation at Safed weather station with a changing emphasis. Overall, PC-8 of the zonal wind component is the determining factor for winter time precipitation of Safed weather station compared to the PCs

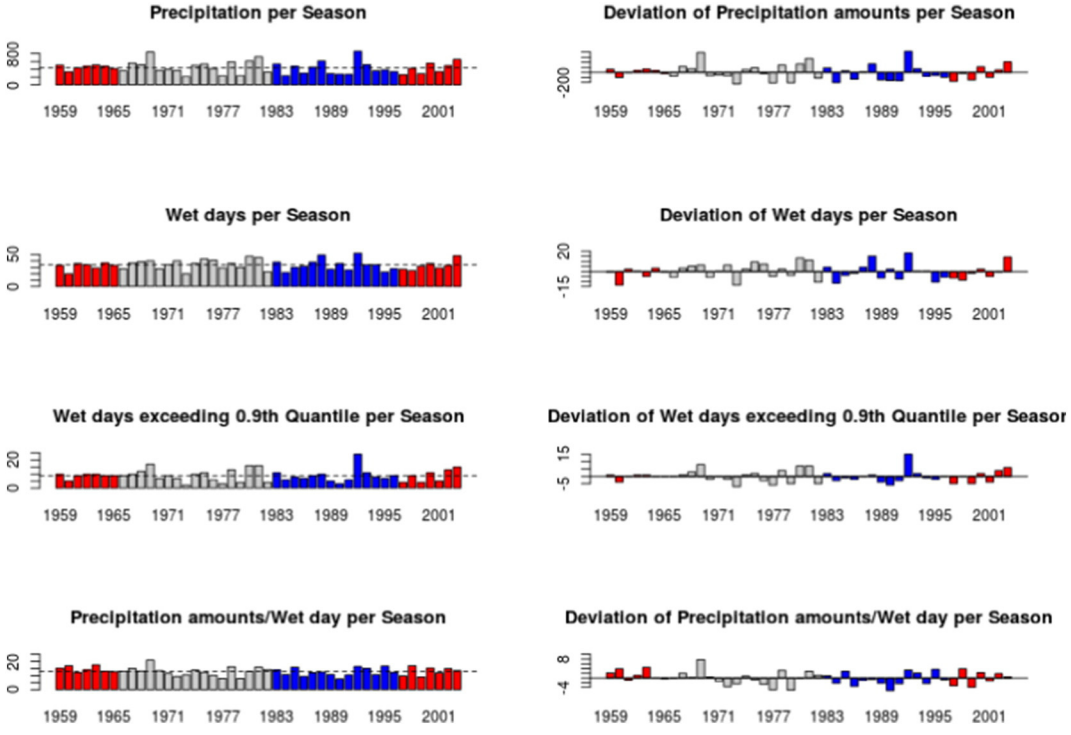

Fig. 3. Precipitation amounts, wet days per season, wet days exceeding the 90th precipitation quantile and precipitation amount per wet day and season for Safed weather station in winter. On the left side the absolute values and on the right side the mean deviation per season are depicted. The colors represent the respective periods (blue: $CQVSS_{MIN}$; red: $CQVSS_{MAX}$; gray: overlapping years). The dashed black lines on the left side represent the mean values. (For interpretation of the references to color in this figure legend, the reader is referred to the web version of this article.)

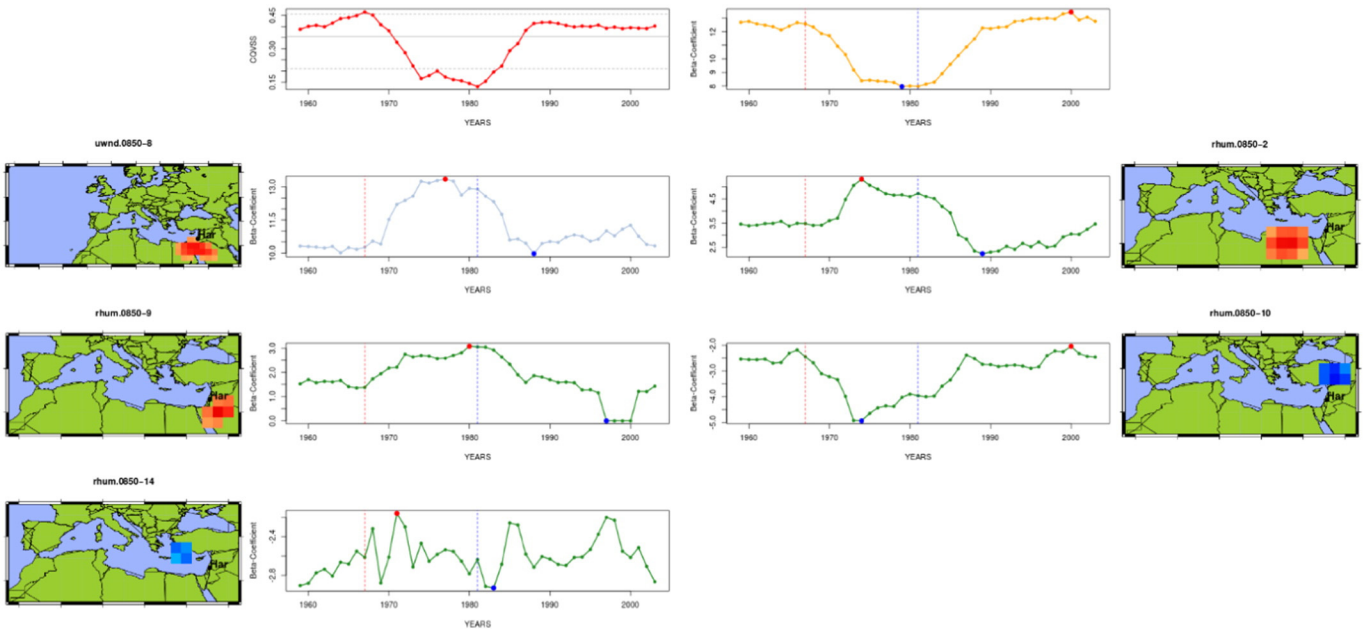

Fig. 4. Censored Quantile Verification Skill Score (CQVSS), beta coefficients and loadings >|0.7| of the respective PCs of Safed weather station for winter season. The figure on the top left shows the CQVSS of the non-stationary model with gray dashed lines for the upper and lower boundary of the range of natural variability and a gray solid line for the mean value. The figure on the top right shows the beta-0 coefficient for the respective subinterval and the bottom figures the beta-coefficients of the respective PC. The location of the corresponding PC is presented beside the beta-coefficients by means of the PC loadings (blue: negative loadings; red: positive loadings). The red (blue) dots mark the period with the highest (lowest) beta-coefficient and the vertical red (blue) dashed lines the periods with the highest (lowest) CQVSS. (For interpretation of the references to color in this figure legend, the reader is referred to the web version of this article.)

of the relative humidity since the mean absolute β-coefficient is higher than the β-coefficients of all other PCs together. Possible effects of the large-scale circulation on non-stationary behavior of precipitation amounts at Safed weather station should be clearly distinct in the composites of this PC.

4.3.2. Statistical model performance and detection of non-stationarities

In Fig. 5 the results of the sliding 31-year subintervals of the BSS and the CQVSS as well as the range of natural variability calculated by means of the 100 random samples are presented for Safed weather station. The upper and lower boundary of both skill scores are represented by blue (lower) and red (upper) dashed lines, the mean of the 100 random samples by a solid gray line. For the BSS the range of natural variability lies between 0.4376 and 0.6506, for the CQVSS between 0.2109 and 0.4565. The estimated skill scores of the validation periods are assigned to the middle year of the calibration periods. Both graphs show almost the same characteristics with high values until the late 1960s followed by a strong decrease with minimum values around 1980. Subsequently, a strong increase of the skill scores takes place until the scores reach a pre-non-stationary level at the end of the 1980s. Noticeable is, that there is a time lag of 1–2 years between the CQVSS and the BSS. Differences can be observed also for the maximum values and the pre- and post-non-stationary level. While the BSS reaches its maximum after the non-stationary period in 1997 (0.6524) and the pre- and post-non-stationary level are almost of the same extent the CQVSS reaches its maximum in front of the non-stationary level and the skill scores of the post-non-stationary level are of smaller, but still high extent in comparison to the pre-non-stationary level. The duration of the strong increase respectively decrease (7–8 years) as well as the rates (±0.03–0.04/a) of both skill scores are rather of the same extent. Overall, a medium negative non-stationarity can be observed for the CQVSS with its minimum in 1981 whereas a large negative non-stationarity with its minimum in 1979 exists for the BSS.

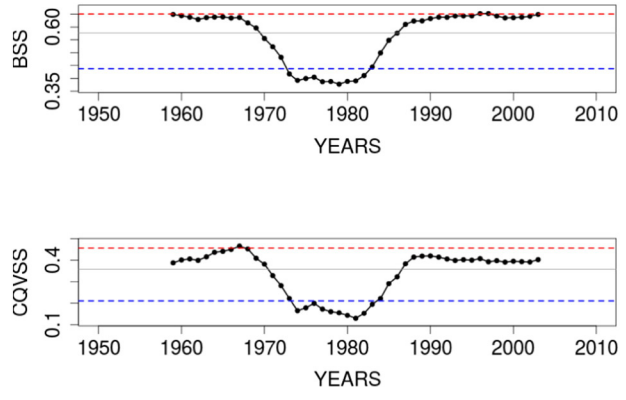

Fig. 5. Brier Skill Score (BSS) and Censored Quantile Verification Skill Score (CQVSS) of the running subinterval for the non-stationary model setup. The range of natural variability is represented by the dashed colored lines and the mean value by a gray solid line.

4.3.3. Analyses of the medium negative non-stationarity of the CQVSS

For further analyses subsamples of the periods with the highest and lowest CQVSS were created. Because of overlapping years, only those years were taken into account which are explicitly part of one subinterval. The period with the highest CQVSS, centered in 1967, contains the years from 1959 to 1982 and 1997–2003, and with the lowest CQVSS, centered in 1981, the years 1966–1996. After removing the overlapping years both periods of Safed weather station contain 14 years, denoted as $CQVSS_{MAX}$ and $CQVSS_{MIN}$ ($CQVSS_{MAX}$: 1959–1965 and 1997–2003; $CQVSS_{MIN}$: 1983–1996).

A summary of both periods is given in Table 1. Overall, there are more wet-days and more wet-days exceeding the 90th quantile within $CQVSS_{MIN}$, but mean precipitation per season is higher in $CQVSS_{MAX}$. On average, 18.9 mm more precipitation on almost one day less can be observed in $CQVSS_{MAX}$. In contrast, the difference in the number of wet-days per season exceeding the 90th quantile is only of smaller extent with +0.1 in $CQVSS_{MIN}$. This leads to the assumption that either the amounts of moderate rain or the amounts of heavy precipitation or both are greater in $CQVSS_{MAX}$. Due to the β-coefficients, all absolute

Table 1
Basic statistics of the rainfall distribution for $CQVSS_{MIN}$ and $CQVSS_{MAX}$.

	$CQVSS_{MIN}$	$CQVSS_{MAX}$
Middle year:	1981	1967
Period:	1983–1996	1959–1965; 1997–2003
Precipitation per season (in mm):	424.8	443.7
Difference (in mm):		+18.9
Wet days per season:	32.5	31.6
Difference:	+0.9	
Wet days $\tau > 0.9$:	8.9	8.8
Difference:	+0.1	
Beta-coefficients:		
Beta-0	+7.98	+12.58
Uwnd.0850 PC-8	+12.90	+10.26
Rhum.0850 PC-2	+4.74	+3.48
Rhum.0850 PC-9	+3.06	+1.38
Rhum.0850 PC-10	−3.97	−2.45
Rhum.0850 PC-14	−2.64	−2.61

values of the coefficients except from β_0 are greater in $CQVSS_{MIN}$ with the highest values for the center of variation of the zonal wind component. Approximately 50% of rainfall variability of both subsamples is caused by PC-8 of the zonal wind component. The unexplained fraction of precipitation (β_0) which cannot be described by the different PCs is of greater extent in $CQVSS_{MAX}$.

Since standard quantile regression (step two and three of TSCQR) is a linear regression the estimated precipitation amounts directly depend on the PC scores (PCS) of the predictors. For this reason high PCS should lead to high estimated rainfall amounts and scores less than zero should estimate zero precipitation, especially when the β-coefficients are as high as the β-coefficient of the zonal wind component. Thus, due to less wet days per season in $CQVSS_{MAX}$ the number of events in the negative tail of the PCS should be higher in the period $CQVSS_{MAX}$ and, due to almost equal numbers of wet days exceeding the 90th quantile the number of events in the high positive tail should be almost equal as well. In matters of the higher seasonal mean precipitation of $CQVSS_{MAX}$ the number of events around zero should be higher in $CQVSS_{MIN}$, respectively the number of events in the extreme positive tail should be higher in $CQVSS_{MAX}$. On the left side of Fig. 6 the number of events subject to the PCS (top and mid left) as well as the differences of both periods (bottom left) are presented. In general, there is a slight shift of the distribution towards higher PCS in $CQVSS_{MIN}$ which implies more wet days and higher seasonal mean precipitation. The difference plot almost confirms the proposed assumption with a higher number of negative scores in $CQVSS_{MAX}$ and a higher number of events around zero in $CQVSS_{MIN}$. Only in the extreme positive tail the results differ from the assumption that the number should rather be equal with a slight tendency to higher numbers in $CQVSS_{MAX}$. However, the distribution of the PCS shows no significant evidence for the non-stationary behavior of $CQVSS_{MIN}$.

More information about the non-stationary behavior of $CQVSS_{MIN}$ is given by the number of wet days related to the PCS of both subsamples (Fig. 6 right). The plot of the differences between $CQVSS_{MIN}$ and $CQVSS_{MAX}$ at the bottom shows a high number of wet days within the negative sector for $CQVSS_{MAX}$, even in the extreme negative tail. This leads to an underestimation of the modeled precipitation compared to the observation of $CQVSS_{MAX}$ when the PCS of PC-8 of the zonal wind component are negative. The lowest PCS, where wet days occur is about −2.5 in $CQVSS_{MAX}$ and −1.25 in $CQVSS_{MIN}$. 35 wet days are assigned to lower PCS in $CQVSS_{MAX}$ before the first wet day occurs in $CQVSS_{MIN}$. Overall, 21% of all wet days are related to PCS less than zero in $CQVSS_{MIN}$, while 42% are related to negative PCS in $CQVSS_{MAX}$. Nearly half of all wet days in $CQVSS_{MAX}$ occur when PCS imply no rain. The same proportion is maintained when PCS thresholds are chosen that equalize rainfall amounts of β_0 ($CQVSS_{MAX}$: −1.2261; $CQVSS_{MIN}$: −0.6186). Almost 30% of days with lower PCS than the threshold are wet days in $CQVSS_{MAX}$ whereas only 15% of days are wet days in $CQVSS_{MIN}$ although the absolute value of the threshold is higher in $CQVSS_{MAX}$.

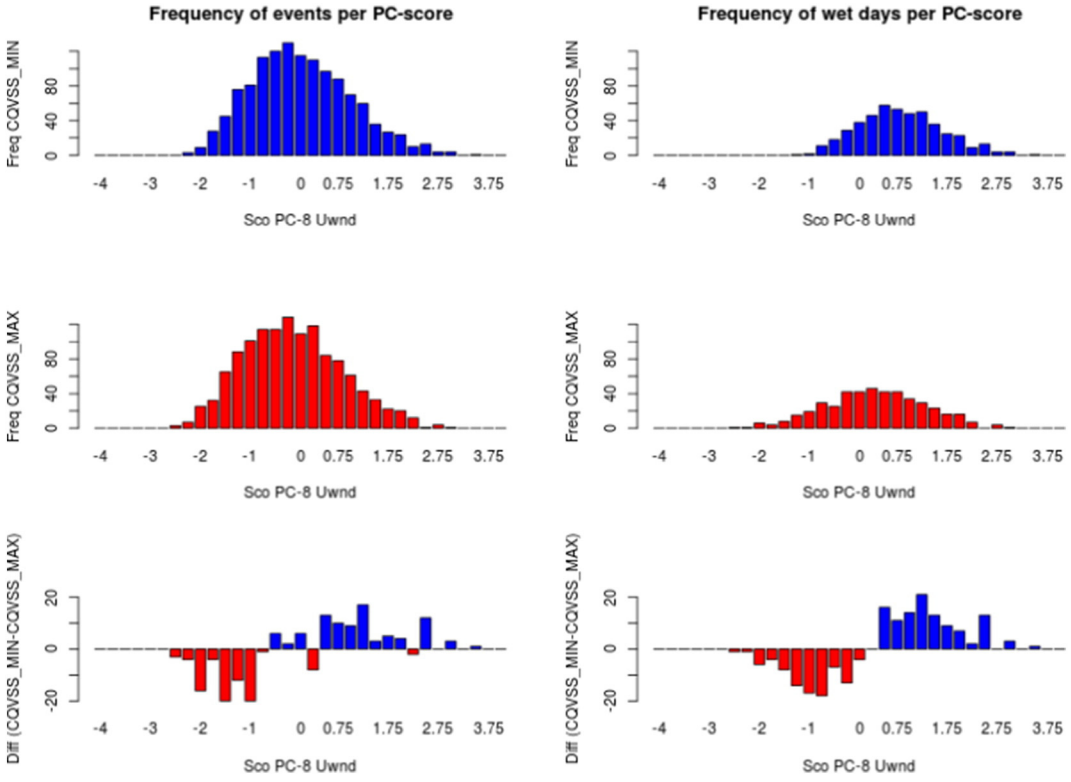

Fig. 6. Frequency of events (left) and wet days (right) per PC score for PC-8 of the zonal wind component at the 850 hPa-level for $CQVSS_{MIN}$ (top) and $CQVSS_{MAX}$ (middle). At the bottom the differences ($CQVSS_{MIN}$-$CQVSS_{MAX}$) are represented. The colors illustrate, whether the number of days is higher in $CQVSS_{MIN}$ (blue) or in $CQVSS_{MAX}$ (red). (For interpretation of the references to color in this figure legend, the reader is referred to the web version of this article.)

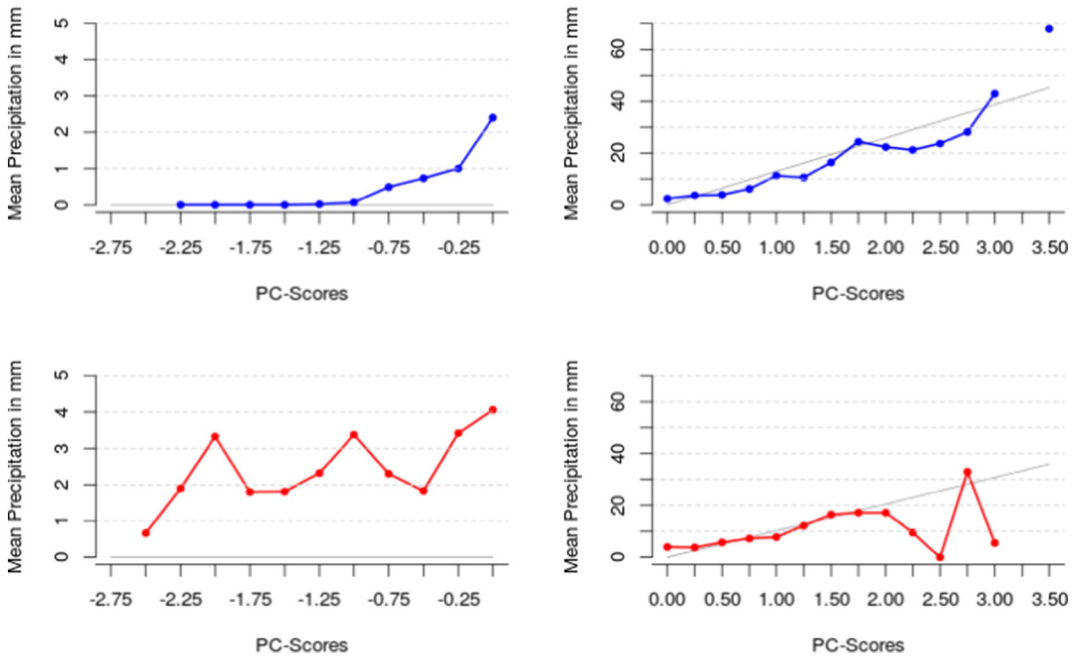

Fig. 7. Modeled Precipitation for the 90th quantile (gray) and observation ($CQVSS_{MIN}$: blue; $CQVSS_{MAX}$: red) per PC score. The modeled precipitation is obtained by the estimated β-coefficient of PC-8 of the zonal wind component. The averaged observed precipitation is centered (±0.125) to the respective PC score of the zonal wind component. (For interpretation of the references to color in this figure legend, the reader is referred to the web version of this article.)

In Fig. 7 the observations and modeled precipitation amounts depending on the PCS are given for both periods. Here, the results for negative scores are presented on the left, the results for positive scores on the right side. For $CQVSS_{MIN}$ (top) the modeled precipitation and the observation show approximately the same development with zero precipitation for the extreme negative PCS, small precipitation amounts for small negative scores and an almost linear increase of observed precipitation for small positive PCS. Only in the extreme positive tail greater differences between observed and modeled precipitation amounts are obtained. The same figure for $CQVSS_{MAX}$ (bottom) shows big differences between modeled and observed precipitation, especially in the negative tail and in the extreme positive tail. Overall, a stronger linear dependency is given for $CQVSS_{MIN}$ in contrast to $CQVSS_{MAX}$ where, to some extent, only in the moderate positive sector linearity is given.

From this it follows that a regression model like $CQVSS_{MIN}$ with a higher linear relationship between modeled and observed precipitation in the calibration period comprehends the predictor-predictand-relationships better than a model like $CQVSS_{MAX}$ but, apparently, it is more prone to changes of the large-scale circulation in the validation period. Because of good results for the moderate positive sector of $CQVSS_{MAX}$ (PCS: 0–2.0) with a high linear relationship the problems are not due to the quantile regression model but due to the first step of the TSCQR since many days with negative PCS are associated with rainfall. The main obstacle of estimating rainfall amounts for Safed weather station is difficulties in modeling rainfall probability. Nevertheless, the model of $CQVSS_{MAX}$ provides better results because it is more stable in matters of changing conditions.

4.3.4. Comparison of composites with PC scores greater/smaller ±2.0 for both periods of Safed weather station

In Table 2 a brief overview is given about the basic statistics which underline previous analyses. Overall, the basic statistics for the extreme negative and positive tail confirm previous results, that the model of $CQVSS_{MAX}$ has a lack of strength in matters of reproducing the calibration period but is more suitable in matters of the transfer to other periods.

The composite means for both periods of the geopotential heights and the wind fields with PCS smaller/greater ±2.0 are shown in Figs. 8 and 9. Here, the large-scale circulation (top), the anomalies (middle) and the wind fields (bottom) of $CQVSS_{MIN}$ are presented on the left, and the results of $CQVSS_{MAX}$ on the right side of the figures for PC-8 of the zonal wind component at the 850 hPa-level (uwnd.0850 PC-8).

In Fig. 8, where the regime anomalies are presented for the composites with PCS <−2.0, a low pressure trough over the the western part of the Mediterranean area surrounded by two high pressure ridges on each side can be observed in both periods. The high pressure system over the eastern part of the Mediterranean basin is responsible for the missing, respectively low precipitation at Safed weather station. In contrast to $CQVSS_{MAX}$, the low pressure system over northwestern Africa is more distinct in $CQVSS_{MIN}$ whereas the high pressure system centered over Cyprus is of smaller extent in terms of strength but of greater extent in terms of size. The center of the low is shifted to the south extending from the Iberian Peninsula over the southern parts of France to southern Germany. The center of the high pressure system over Cyprus is slightly shifted to the west but affects the whole eastern part of

Table 2
Basic statistics of the composite with PC scores <−2.0 (top) and PC scores >+2.0 (bottom) for $CQVSS_{MIN}$ and $CQVSS_{MAX}$.

−	$CQVSS_{MIN}$	$CQVSS_{MAX}$
Beta-coefficient:	12.90	10.26
Events:	5	20
In %:	0.4	1.6
Number of wet days:	0	5
In %:	0.0	25.0
Precipitation/event:	0.0	3.5
Precipitation/wet day	0.0	14.1
+		
Events:	48	25
In %:	3.8	1.98
Number of wet days:	46	17
In %:	95.8	68.0
Precipitation/event:	25.3	16.3
Precipitation/wet day:	26.4	24.0

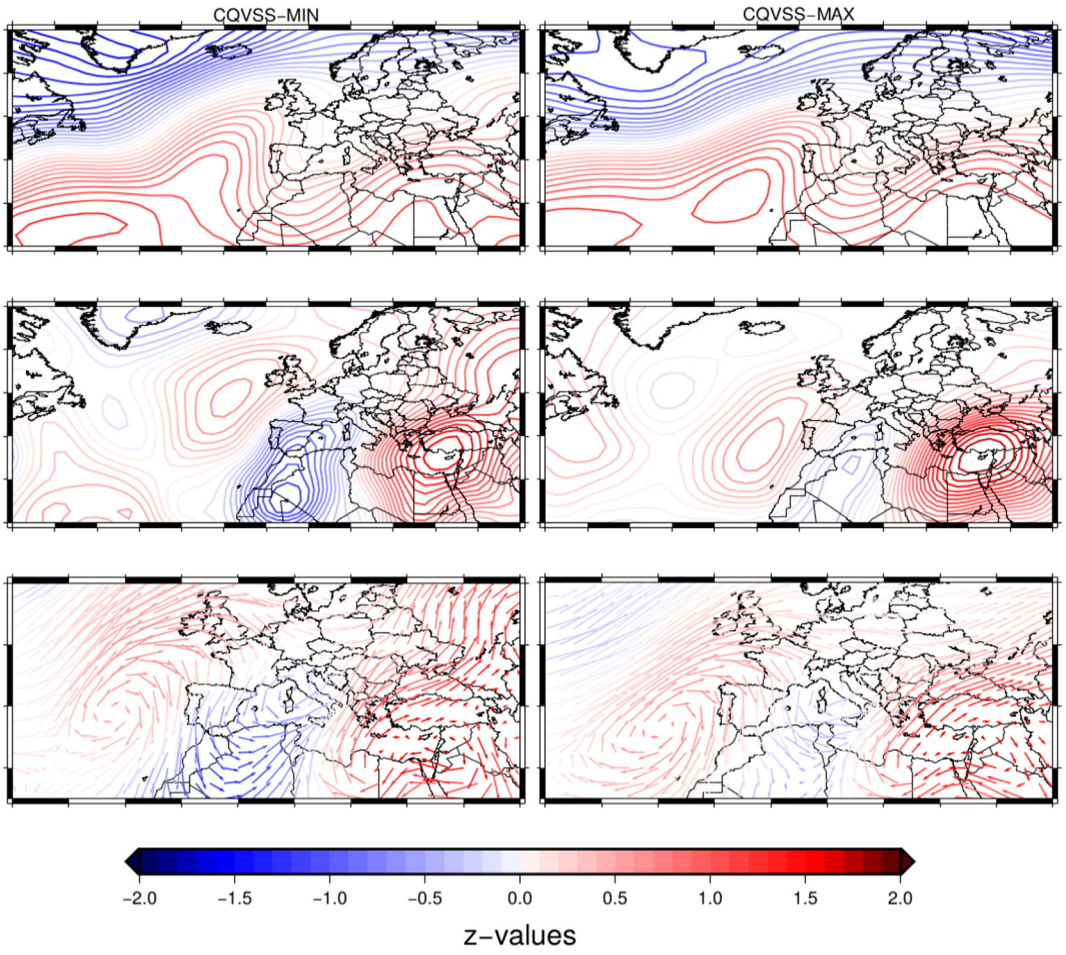

Fig. 8. Composite means for days with PC scores <− 2.0 of uwnd.0850 PC-8 for $CQVSS_{MIN}$ (left) and $CQVSS_{MAX}$ (right). The figures at the top represent the standardized large-scale circulation, the middle figures the anomalies of the geopotential heights at the 850 hPa-level. At the bottom the wind field for the periods $CQVSS_{MIN}$ (left) and $CQVSS_{MAX}$ (right) are illustrated. The colors of the arrows at the bottom are adopted from the anomalies (middle). (For interpretation of the references to color in this figure legend, the reader is referred to the web version of this article.)

Europe as well as the eastern parts of the Mediterranean. In $CQVSS_{MIN}$ the pressure gradient between the Western and Eastern Mediterranean area, representing the negative mode of the Mediterranean Oscillation (MO) lead to stronger southern subtropical airflow with increasing precipitation at coasts exposed to the south/southwest in the Balkans, Greece and Turkey, whereas the Levant is dominated by easterly dry winds of the Arabian Peninsula. According to Alpert et al. (2004) and Saaroni et al. (2010) the pressure difference between the pressure system and its surroundings is not only more essential for cyclonic, but also for anticyclonic conditions than the pressure within the system itself. Furthermore, due to the location of the high pressure system over Cyprus which imparts masses of dry air from the Arabian Peninsula to Israel, the mean wind speed of $CQVSS_{MIN}$ is greater than in $CQVSS_{MAX}$. Hence, the probability of rain caused by small-scale processes is higher in $CQVSS_{MAX}$, since they are less superimposed by the large-scale circulation and, thus, lead to a lack of skill in modeling precipitation amounts for the negative tail of PCS.

Regime anomalies for PCS >+2.0 are presented in Fig. 9. A high pressure ridge over the western part and a low pressure trough over the eastern part are dominant in both periods (Fig. 9 top). A second low pressure system to the west of the high pressure ridge with anomalies of smaller extent is centered over the south-eastern North Atlantic. The center of the high pressure system in $CQVSS_{MIN}$ is placed over the border area of Algeria and Tunisia and extends to northern Scotland, whereas in $CQVSS_{MAX}$ no real center can be determined since it is divided into two shallower cores, which are located over the English Channel and southern Algeria (Fig. 9 middle).

The center of the Cyprus low over the Levant region in $CQVSS_{MIN}$, which is responsible for 90% of the annual precipitation amounts in Israel (Goldreich, 2003), is more deep but slightly shifted to the south, closer to Safed weather station, whereby the mean westerly airflow is smaller than in $CQVSS_{MAX}$. However, by reason of the stronger pressure difference between the Western and Eastern Mediterranean in $CQVSS_{MIN}$, which represents a positive phase of the MO (Conte et al., 1989), more cool air from Eastern Europe reaches the warmer Mediterranean where it becomes moist and unstable (Shay-El and Alpert, 1991) and leads to rainfalls over the Levant. Several studies discussed the relationships of the northerly to westerly winds within a positive mode of the MO with Israeli rainfall amounts (e.g. Kutiel et al., 1996; Krichak et al., 2000; Dünkeloh and Jacobeit, 2003) and came to the conclusion, that the Eastern Mediterranean (EM) upper-level trough is the major synoptic-scale factor of rainfall in Israel (Ziv et al., 2006).

Furthermore, due to the positive mode of the MO, the mean wind speeds over the western and central parts of the Mediterranean basin are higher in $CQVSS_{MIN}$ (Fig. 9 bottom), so that there is an increase of the number of cyclones which originate in the Western Mediterranean (WM), especially in the Gulf of Genoa and the Atlas lee region, and which reach the eastern parts of the Mediterranean. Here, a deepening and rejuvenation of existing cyclones in the Cyprus area takes place (Goldreich, 2003). Since the interannual variation of the cyclone occurrence is responsible for ~50% of the rainfall variability in the Levant region (Saaroni et al., 2010), the number of cyclones could be a possible explanation of non-stationary behavior in the predictor-predictand-relationships. Flocas et al. (2010) evaluates the number of cyclones which

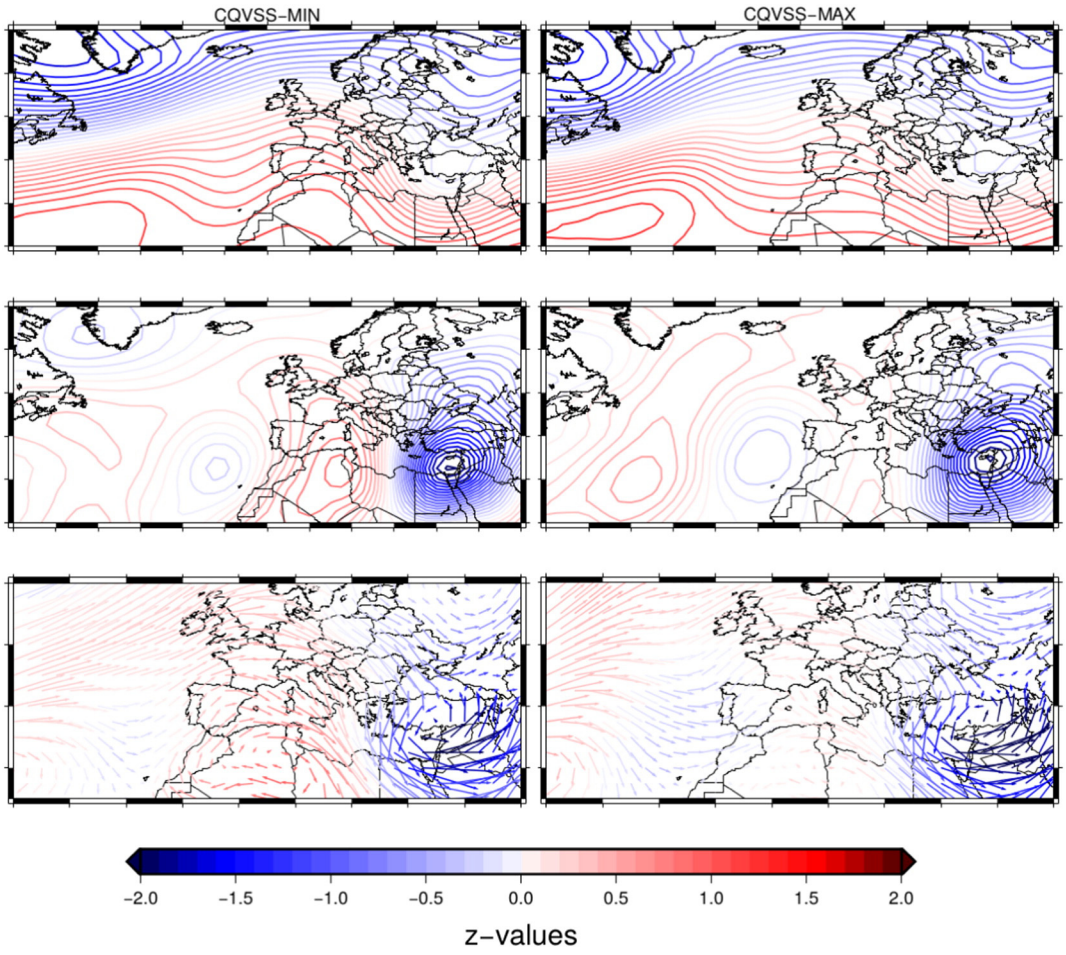

Fig. 9. Same as Fig. 8 but for composite means for days with PC scores >+2.0.

affect rainfall in the EM due to its origins, seasonal distribution and annual trends. Most of the cyclones imparting rain to Israel originate in the EM with a significant positive trend over the second half of the 20th century, whereas cyclones with origins outside the EM exhibit a significant decreasing trend. Overall, the number of cyclones over the EM decreases in winter season since the increasing number of cyclones originates in the EM cannot compensate the lack of cyclones passing from other regions. Since PC-8 of the zonal wind component is located over Egypt and the Arabian Peninsula, decisive processes, especially in the central and western parts of the Mediterranean, cannot be comprised by this center of variation. Thus, even if the center of variation is of the same extent in both periods, it cannot capture the lack of moisture transport by a decreasing number of cyclones passing from other regions.

Another reason for the differences between $CQVSS_{MAX}$ and $CQVSS_{MIN}$ is related to the location of the Cyprus lows which is essential for the trajectory of the winds entering Israel. Especially the trajectory over the Mediterranean Sea determines the moisture content of the air masses and, therefore, the precipitation amounts over the Levant region (Saaroni et al., 2010). Saaroni et al. (2010) found out, that deep lows north or south of Cyprus produce the highest amounts of daily rainfall in northern Israel, whereas lows located to the south of Cyprus are rare and, thus, contribute only a small fraction of seasonal rainfall amounts. Furthermore, by means of correlation analyses of the different types of lows with seasonal rainfall over Israel, the authors showed, that deep lows have the highest correlations with the northeastern region of Israel with decreasing coefficients in southwest direction and vice versa for shallow lows. However, the anomalies of the composites in $CQVSS_{MIN}$ (Fig. 9 middle) show a deep low centered south of Cyprus and a shallower low centered between Cyprus and the Levant coast in $CQVSS_{MAX}$. The rare situation in the second half of the 20th century with deep lows centered south of Cyprus is the normal state within the composites of PCS >2.0 in $CQVSS_{MIN}$. Although the frequency of shallow lows north of Israel, as seen in $CQVSS_{MAX}$, is significantly higher in the second half of the 20th century than the synoptic situation in $CQVSS_{MIN}$, the percentage of rain days for the entire territory of Israel is smaller. Under consideration of the results of the correlation analyses and the percentage of wet days for the different types of lows, the probability of rain is higher in $CQVSS_{MIN}$. These results are in accordance with the numerical evaluation of Table 2, were the probability of rain as well as the precipitation amounts per wet day are higher in $CQVSS_{MIN}$.

In general, the Mediterranean Oscillation is responsible for the rainfall distribution all over the Mediterranean area and, thus, has great influence on the precipitation amounts in the Levant region. But since only small shifts of the Cyprus low can lead to significant changes in the rainfall distribution between the northern and southern parts of Israel and since the number of cyclones which pass the EM from other regions play an important role due to moisture transport, a combination of all three factors is responsible for the non-stationary behavior between the large-scale circulation and heavy precipitation events at Safed weather station.

5. Discussion and conclusion

A Three-step censored quantile regression (TSCQR) was used to statistically downscale heavy precipitation events in the Mediterranean area. Different variables of the 850 hPa- and 700 hPa-level were used

as predictors and the seasonal time series of 94 weather stations were used as predictands to estimate the 90th quantile of precipitation. Overall, the Brier Skill Score (BSS), which was used to assess the skill of the logit models, and the Censored Quantile Verification Skill Score (CQVSS), which was used to assess the skill of the quantile regression models, have shown, that the TSCQR is appropriate to model heavy precipitation events.

The selection of the significant centers of variations was based on two steps. First, by means of reproducing the whole time series, the combination of two variables with the best model performance was determined for all reference stations. Under consideration of a third predictor variable the CQVSS shows only little improvements. Subsequently, the number of significant PCs was determined by means of estimating 100 31-year random samples. If a PC was significant in 95% of all cases the PC was taken into account for further analyses. A higher threshold resulted in only one PC for some stations, and smaller thresholds led to the problem of overfitting due to a high number of significant PCs.

Non-stationary behavior in the statistical model performance was detected by comparing the BSS and the CQVSS of running sub-intervals of 31 years with scores of 100 random samples, with the highest and lowest score determining the range of natural variability. About 40% of all reference stations show non-stationary behavior in the statistical model performance of variable duration. Negative non-stationarities, where the scores of the running subintervals fall below the lower boundary of the range of natural variability, mainly occur in the eastern Mediterranean, whereas positive non-stationarities, where the scores of the running subintervals exceeds the upper boundary, mainly occur in the western Mediterranean.

If a time series was affected by non-stationary behavior in the predictor-predictand-relationships, composite means were calculated for all PCs of the sub-intervals with the highest and lowest CQVSS after removing the overlapping years. Only those days were taken into account, where the respective PCS exceed a certain threshold. Subsequently, a numerical evaluation of both periods was performed, followed by comparisons of the composite means of the large-scale circulation, the anomalies of the geopotential heights and the wind fields.

By means of the reference station of precipitation region 2 the method and results were illustrated. The daily precipitation time series of Safed exhibits a distinct non-stationarity in the mid-seventies to early eighties. The censored quantile regression model is based on five different PCs of the zonal wind component and the relative humidity of the 850 hPa-level. Here, PC-8 of the zonal wind component is the most important center of variation for the 90th precipitation quantile of Safed weather station. The β-coefficient of the zonal wind component is as twice as high as all other β-coefficients together and for this reason non-stationary behavior in the predictor-predictand-relationships should trace back to this PC. Thus, the evaluation and the comparison of composites means of all days with PC scores smaller/greater ± 2.0 was only executed for the PC of the zonal wind component.

The evaluation showed, that the relationships between the center of variation and the 90th quantile of precipitation at Safed weather station is more distinct in the period $CQVSS_{MIN}$, where we received the lowest CQVSS. In the period $CQVSS_{MAX}$ there is a great number of wet days although the PCS imply no rain, in contrast to $CQVSS_{MIN}$ where the modeled precipitation amounts and the observations are in good agreement. For this reason we came to the conclusion, that a good regression model, which comprises the conditions of the calibration period quite good, is not always transferable to other periods, because the large-scale circulation has changed.

In order to find reasons for non-stationary behavior within the different sub-periods we compared the composite means of the large-scale circulation, the anomalies and the wind field of both periods. Three possible reasons were discussed within the case study using Safed weather station. The MO was determined as one of the major factors for the non-stationary behavior. For PCS <–2.0 as well as for PCS >+2.0 the MO is more distinct in the period $CQVSS_{MIN}$, with the respective pressure system over the EM being very pronounced in both periods. However, the pressure systems over the WM exhibit clear differences in matters of strength, since they are well developed in $CQVSS_{MIN}$ and only barely present in $CQVSS_{MAX}$. The different characteristics of the MO impact on the location of the pressure system over the EM as well as on the cyclone tracks over the Mediterranean basin. Due to a weaker MO in $CQVSS_{MAX}$ the moisture transport by cyclones from the WM is limited, since the number of cyclones originating in the WM, which pass the EM, decreases. The increase of cyclone activity in the EM cannot compensate the lack of moisture passing from the WM. Furthermore, the location of the pressure system over the EM in $CQVSS_{MIN}$ is slightly shifted to the west in both cases. Thus, there are weaker dry winds from the Arabian Peninsula for the composite means with PCS <-2.0 in $CQVSS_{MAX}$, so that small scale processes gain more influence at Safed weather station. In the opposite case a deep Cyprus low is located south of Cyprus in $CQVSS_{MIN}$, which leads to increasing rainfall amounts over the northern Levant region, whereas a shallow Cyprus low provides unstable precipitation amounts at Safed weather station in $CQVSS_{MAX}$.

The present study shows, that changes of the large-scale circulation can affect the quality of regression models. Thus, there is a great need to consider those non-stationary behaviors of the large-scale circulation within the scope of statistical downscaling in order to obtain an improvement of the assessments of future climate change. Since this study demonstrates that this method is applicable for any precipitation quantile of interest in winter, an extension to the transitional seasons should be considered as well, because the contribution of precipitation extremes in the transitional seasons cannot be disregarded due to the annual water budget of the Mediterranean area.

References

Alexandersson, H., 1986. A homogeneity test applied to precipitation data. J. Climatol. 6, 661–675. http://dx.doi.org/10.1002/joc.3370060607.

Alpert, P., Ben-Gai, T., Baharad, A., Benjamini, Y., Yekutieli, D., Colacino, M., Diodato, L., Ramis, C., Homar, V., Romero, R., Michaelides, S., Manes, A., 2002. The paradoxical increase of Mediterranean extreme daily rainfall in spite of decrease in total values. Geophys. Res. Lett. 29 (10), 31-1–31-4. http://dx.doi.org/10.1029/2001GL013554.

Alpert, P., Osetinsky, I., Ziv, B., Shafir, H., 2004. Semi-objective classification for daily synoptic systems, application to the Eastern Mediterranean climate change. Int. J. Climatol. 24 (8), 1013-1011. http://dx.doi.org/10.1002/joc.1036.

Barkhordarian, A., von Storch, H., Bhend, J., 2013. The expectation of future precipitation change over the Mediterranean region is different from what we observe. Clim. Dyn. 40 (1–2), 225–244. http://dx.doi.org/10.1007/s00382-012-1497-7.

Batllori, E., Parisien, M.-A., Krawchuk, M.A., Moritz, M.A., 2013. Climate change-induced shifts in fire for Mediterranean ecosystems. Glob. Ecol. Biogeogr. 22, 1118–1129. http://dx.doi.org/10.1111/geb.12065.

Beck, C., Jacobeit, J., Jones, P.D., 2007. Frequency and within-type variations of large-scale circulation types and their effects on low-frequency climate variability in Central Europe since 1780. Int. J. Climatol. 27 (4), 473–491. http://dx.doi.org/10.1002/joc.1410.

Bremnes, J.B., 2004. Probabilistic forecasts of precipitation in terms of quantiles using NWP model output. Mon. Weather Rev. 132 (1), 338–347. http://dx.doi.org/10.1175/1520-0493(2004)132<0338:PFOPIT>2.0.CO;2.

Chernozhukov, V., Hong, H., 2002. Three-step censored quantile regression and extramarital affairs. J. Am. Stat. Assoc. 97 (458), 872–882. http://dx.doi.org/10.1198/016214502388618663.

Conte, M., Giuffrida, S., Tedesco, S., 1989. The Mediterranean Oscillation: impact on precipitation and hydrology in Italy. Conf. Clim. Water 1, 121–137.

Dünkeloh, A., Jacobeit, J., 2003. Circulation dynamics of Mediterranean precipitation variability 1948–98. Int. J. Climatol. 23 (15), 1843–1866. http://dx.doi.org/10.1002/joc.973.

Fernandez, J., Saenz, J., Zorita, E., 2003. Analysis of wintertime atmospheric moisture transport and its variability over southern Europe in the NCEP Reanalyses. Clim. Res. 23 (3), 195–215.

Filipe, A.F., Lawrence, J.E., Bonada, N., 2013. Vulnerability of stream biota to climate change in mediterraneanclimate regions: a synthesis of ecological responses and conservation challenges. Hydrobiologia 719, 331–351. http://dx.doi.org/10.1007/s10750-012-1244-4.

Fitzenberger, B., 1997. A guide to censored quantile regressions. Handbook of Statistics vol. 15, pp. 405–437.

Flocas, H.A., Simmonds, I., Kouroutzoglou, J., Keay, K., Hatzaki, M., Bricolas, V., Asimakopoulos, D., 2010. On cyclonic tracks over the eastern Mediterranean. J. Clim. 23 (19), 5243–5257. http://dx.doi.org/10.1175/2010JCLI3426.1.

Friederichs, P., 2010. Statistical downscaling of extreme precipitation events using extreme value theory. Extremes 13 (2), 109–132. http://dx.doi.org/10.1007/s10687-010-0107-5.

Friederichs, P., Hense, A., 2007. Statistical downscaling of extreme precipitation events using censored quantile regression. Mon. Weather Rev. 135 (6), 2365–2378. http://dx.doi.org/10.1175/MWR3403.1.

Friederichs, Hense, 2008. A probabilistic forecast approach for daily precipitation totals. Weather Forecast. 23 (4), 659–673. http://dx.doi.org/10.1175/2007WAF2007051.1.

Gao, X., Pal, J.S., Giorgi, F., 2006. Projected changes in mean and extreme precipitation over the Mediterranean region from a high resolution double nested RCM simulation. Geophys. Res. Lett. 33 (3), L03706. http://dx.doi.org/10.1029/2005GL024954.

Giorgi, F., 2006. Climate change hot-spots. Geophys. Res. Lett. 33 (8), L08707. http://dx.doi.org/10.1029/02006GL025734.

Giorgi, F., Lionello, P., 2008. Climate change projections for the Mediterranean region. Glob. Planet. Chang. 63, 90–104. http://dx.doi.org/10.1016/j.glopacha.2007.09.005.

Glahn, H.R., Lowry, D.A., 1972. The use of model output statistics (MOS) in objective weather forecasting. J. Appl. Meteorol. 11 (8), 1203–1211. http://dx.doi.org/10.1175/1520-0450(1972)011<1203:TUOMOS>2.0.CO;2.

Goldreich, Y., 2003. The Climate of Israel: Observation, Research and Application Springer Science & Business Media.

Henne, P.D., Elkin, C., Colombaroli, D., Samartin, S., Bugmann, H., Heiri, O., Tinner, W., 2013. Impacts of changing climate and land use on vegetation dynamics in a Mediterranean ecosystem: insights from paleoecology and dynamic modeling. Landsc. Ecol. 28 (5), 819–833. http://dx.doi.org/10.1007/s10980-012-9782-8.

Hertig, E., Jacobeit, J., 2013. A novel approach to statistical downscaling considering nonstationarities: application to daily precipitation in the Mediterranean area. J. Geophys. Res. Atmos. 118 (2), 520–533. http://dx.doi.org/10.1002/jgrd.50112.

Hertig, E., Jacobeit, J., 2014. Considering observed and future nonstationarities in statistical downscaling of Mediterranean precipitation. Theor. Appl. Climatol. 1–17 http://dx.doi.org/10.1007/s00704-014-1314-9.

Hertig, E., Seubert, S., Paxian, A., Vogt, G., Paeth, H., Jacobeit, J., 2012. Changes of total versus extreme precipitation and dry periods until the end of the 21st century: statistical assessments for the Mediterranean area. Theor. Appl. Climatol. 111 (1–2), 1–20. http://dx.doi.org/10.1007/s00704-012-0639-5.

Hertig, E., Seubert, S., Paxian, A., Vogt, G., Paeth, H., Jacobeit, J., 2014. Statistical modeling of extreme precipitation indices for the Mediterranean area under future climate change. Int. J. Climatol. 34 (4), 1132–1156. http://dx.doi.org/10.1002/joc.3751.

Iglesias, A., Rosenzweig, C., Pereira, D., 2007. Agricultural impacts of climate change in Spain: developing tools for spatial analysis. Glob. Environ. Chang. 10 (1), 69–80.

Kalnay, E., Kanamitsu, M., Kistler, R., Collins, W., Deaven, D., Gandin, L., Iredell, M., Saha, S., White, G., Woollen, J., Zhu, Y., Leetmaa, A., Reynolds, R., Chelliah, M., Ebisuzaki, W., Higgins, W., Janowiak, J., Mo, K.C., Ropelewski, C., Wang, J., Jenne, R., Joseph, D., 1996. The NCEP/NCAR 40-year reanalysis project. Bull. Am. Meteorol. Soc. 77 (3), 437–471. http://dx.doi.org/10.1175/1520-0477(1996)077<0437:TNYRP>2.0CO;2.

Kelley, C., Ting, M., Seager, R., Kushnir, Y., 2012. The relative contributions of radiative forcing and internal climate variability to the late 20th century winter drying of the Mediterranean region. Clim. Dyn. 38 (9–10), 2001–2015. http://dx.doi.org/10.1007/s00382-011-1221-z.

Kistler, R., Kalnay, E., Collins, W., Saha, S., White, G., Woollen, J., Chelliah, M., Ebisuzaki, W., Kanamitsu, M., Kousky, V., van den Dool, H., Jenne, R., Fiorino, M., 2001. The NCEP/NCAR 50-year reanalysis: monthly means CD-ROM and documentation. Bull. Am. Meteorol. Soc. 82, 247–267. http://dx.doi.org/10.1175/1520-0477(2001)082>0247:TNNYRM>2.3CO;2.

Klein, W.H., 1971. Computer prediction of precipitation probability in the United States. J. Appl. Meteorol. 10 (5), 903–915. http://dx.doi.org/10.1175/1520-0450(1971)010<0903:CPOPPI>2.0.CO:2.

Klein Tank, A.M.G., Wijngaard, J.B., Können, G.P., Böhm, R., Demaree, G., Gocheva, A., Mileta, M., Pashiardis, S., Hejkrlik, L., Kern-Hansen, C., Heino, R., Bessemoulin, P., Müller-Westermeier, G., Tzanakou, M., Szalai, S., Palsdottir, T., Fitzgerald, D., Rubin, S., Capaldo, M., Maugeri, M., Leitass, A., Bukantis, A., Aberfeld, R., van Engelen, A.F.V., Forland, E., Mietus, M., Coelho, F., Mares, C., Razuvaev, V., Nieplova, E., Cegnar, T., Antonio Lopez, J., Dahlström, B., Moberg, A., Kirchhofer, W., Ceylan, A., Pachaliuk, O., Alexander, L.V., Petrovic, P., 2002. Daily dataset of 20th-century surface air temperature and precipitation series for the European Climate Assessment. Int. J. Climatol. 22 (12), 1441–1453. http://dx.doi.org/10.1002/joc.773.

Koenker, R., 2005. Quantile regression. No. 38. Cambridge university press.

Koenker, R., 2013. Quantreg: quantile regression. R package version 5.05.

Koenker, R., Bassett, B., 1978. Regression quantiles. Econometrica 46 (1), 33–50. http://dx.doi.org/10.2307/1913643.

Krichak, S.O., Tsidulko, M., Alpert, P., 2000. Monthly synoptic patterns associated with wet/dry conditions in the eastern Mediterranean. Theor. Appl. Climatol. 65 (3–4), 215–229. http://dx.doi.org/10.1007/s007040070045.

Kunstmann, H., Heckl, A., Rimmer, A., 2006. Physically based distributed hydrological modelling of the Upper Jordan catchment and investigation of effective model equations. Adv. Geosci. 9, 123–130.

Kutiel, H., Maheras, P., Guika, S., 1996. Circulation and extreme rainfall conditions in the eastern Mediterranean during the last century. Int. J. Climatol. 16 (1), 73–92. http://dx.doi.org/10.1002/(SICI)1097-088(199601)16:1<73:AID-JOC997>3.0.CO:2-G.

Latorre, J.G., Garcia-Latorre, J., Sanchez-Picon, A., 2001. Dealing with aridity: socio-economic structures and environmental changes in an arid Mediterranean region. Land Use Policy 18 (1), 53–64. http://dx.doi.org/10.1016/S0264-8377(00)00045-4.

Lionello, P., Abrantes, F., Gacic, M., Planton, S., Trigo, R., Ulbrich, U., 2014. The climate of the Mediterranean region: research progress and climate change impacts. Reg. Environ. Chang. 14 (5), 1679–1684. http://dx.doi.org/10.1007/s10113-014-0666-0.

Maccracken, M.C., Barron, E.J., Easterling, D.R., Felzer, B.S., Karl, T.R., 2003. Climate change scenarios for the US National Assessment. Bull. Am. Meteorol. Soc. 84 (12), 1711–1723. http://dx.doi.org/10.1175/BAMS-84-12-1711.

Mariotti, A., Dell'Aquila, A., 2012. Decadal climate variability in the Mediterranean region: roles of large-scale forcings and region processes. Clim. Dyn. 38 (5–6), 1129–1145. http://dx.doi.org/10.1007/s00382-011-1056-7.

Martius, O., Schwierz, C., Davies, H.C., 2008. Far-upstream precursors of heavy precipitation events on the alpine south-side. Q. J. R. Meteorol. Soc. 134 (631), 417–428.

Marzban, C., Sandgathe, S., Kalnay, E., 2006. MOS, perfect prog, and reanalysis. Mon. Weather Rev. 134 (2), 657–663. http://dx.doi.org/10.1175/MWR3088.1.

Massacand, A., Wernli, H., Davies, H.C., 1998. Heavy precipitation on the Alpine southside: an upper level precursor. Geophys. Res. Lett. 25 (9), 1435–1438.

Moberg, A., Jones, P.D., 2005. Trends in indices for extremes in daily temperature and precipitation in Central and Western Europe, 1901–99. Int. J. Climatol. 25 (9), 1149–1172. http://dx.doi.org/10.1002/joc.1163.

Moberg, A., Jones, P.D., Lister, D., Walther, A., Brunet, M., Jacobeit, J., Alexander, L.V., Della-Marta, P.M., Luterbacher, J., Yiou, P., Chen, D., Klein Tank, A.M.G., Saladie, O., Sigro, J., Aguilar, E., Alexandersson, H., Almarza, C., Auer, I., Barriendos, M., Begert, M., Bergström, H., Böhm, R., Butler, C.J., Caesar, J., Drebs, A., Founda, D., Gerstengarbe, F.-W., Micela, G., Maugeri, M., Österle, H., Pandzic, K., Petrakis, M., Srnec, L., Tolasz, R., Tuomenvirta, H., Werner, P.C., Linderholm, H., Philipp, A., Wanner, H., Xoplaki, E., 2006. Indices for daily temperature and precipitation extremes in Europe analyzed for the period 1901–2000. J. Geophys. Res. Atmos. 111 (D22). http://dx.doi.org/10.1029/2006JD007103 (1984-2012).

Preisendorfer, R.W., 1988. In: Mobley, C.D. (Ed.)Principal Component Analysis in Meteorology and Oceanography vol. 425. Elsevier, Amsterdam.

Richman, M.B., 1986. Rotation of principal components. J. Climatol. 6, 293–335.

Saaroni, H., Halfon, N., Ziv, B., Alpert, P., Kutiel, H., 2010. Links between the rainfall regime in Israel and location and intensity of Cyprus lows. Int. J. Climatol. 30 (7), 1014–1025. http://dx.doi.org/10.1002/joc.1912.

Shay-El, Y., Alpert, P., 1991. A diagnostic study of winter diabatic heating in the Mediterranean in relation to cyclones. Q. J. R. Meteorol. Soc. 117 (500), 715–747. http://dx.doi.org/10.1002/qj.49711750004.

Stefanova, A., Hesse, C., Krysanova, V., 2015. Combined impacts of medium term socio-economic changes and climate change on water resources in a managed Mediterranean catchment. Water 7 (4), 1538–1567. http://dx.doi.org/10.3390/w7041538.

Toreti, A., Naveau, P., 2015. On the evaluation of climate model simulated precipitation extremes. Environ. Res. Lett. 10 (1), 014012.

Toreti, A., Giannakaki, P., Martius, O., 2015. Precipitation extremes in the Mediterranean region and associated upper-level synoptic-scale flow structures. Clim. Dyn. 1–17 http://dx.doi.org/10.1007/s00382-015-2942-1.

Wijngaard, J.B., Klein Tank, A.M.G., Können, G.P., 2003. Homogeneity of 20th century European daily temperature and precipitation series. Int. J. Climatol. 23 (6), 679–692. http://dx.doi.org/10.1002/joc.906.

Wilks, D.S., 2011. Statistical Methods in the Atmospheric Sciences vol. 100. Academic Press.

Xoplaki, E., Gonzalez-Rouco, J.F., Luterbacher, J.U., Wanner, H., 2004. Wet season Mediterranean precipitation variability: influence of large-scale dynamics and trends. Clim. Dyn. 23 (1), 63–78. http://dx.doi.org/10.1007/s00382-004-0422-0.

Ziv, B., Dayan, U., Kushnir, Y., Roth, C., Enzel, Y., 2006. Regional and global atmospheric patterns governing rainfall in the southern Levant. Int. J. Climatol. 26 (1), 55–73. http://dx.doi.org/10.1002/joc.1238.